Available online at www.sciencedirect.com

ScienceDirect

Ceramics International 39 (2013) 9567–9574

CERAMICS INTERNATIONAL

www.elsevier.com/locate/ceramint

Effect of zirconium diboride addition on the properties of silicon carbide composites

M. Sai Krupa[a], N. Dileep Kumar[a], R. Suresh Kumar[b], P. Chakravarthy[a,*], Karodi Venkateswarlu[c]

[a]Department of Aerospace Engineering, Indian Institute of Space Science and Technology, India
[b]Materials and Metallurgy Group, Vikram Sarabhai Space Centre, India
[c]National Aerospace Laboratories, India

Received 22 March 2013; received in revised form 18 May 2013; accepted 18 May 2013
Available online 25 May 2013

Abstract

SiC and its composites have large potential in the aerospace sector due to their inherent advantages. However, the beneficial properties of high hardness and high strength of SiC cause problems in fabricating these composites by machining. Electro discharge machining (EDM) is found to be reliable technique to machine such hard materials and demands the work material to be conductive. Thus the present work focuses on synthesizing SiC composite with 10, 20, 30 vol% zirconium diboride (ZrB_2) as reinforcement to study the physical and mechanical properties and its machinability by EDM. SiC and its composites were vacuum hot pressed at 1900 °C to near theoretical densities. It was observed that with the addition of ZrB_2, hardness of the composite increased while the flexural strength decreased and the electrical resistivity decreased with increase of ZrB_2 content. Feasibility studies of machining the composites with EDM were carried out and the experiments showed that SiC–30 vol% ZrB_2 composite alone could be machined. This revealed that this composite possessed adequate conductivity for carrying out EDM.

Keywords: A. Hot pressing; Electro discharge machining; SiC–ZrB_2 composite; Machinability

1. Introduction

Progress in materials processing and manufacturing requires research on processing, microstructural aspects and their interaction to achieve desired final properties. Research towards the fundamental understanding of the processing and behavior support the industrial need for materials in automotive, aerospace and other applications. Materials with low density, good mechanical strength and high oxidation resistance at elevated temperatures (>1500 °C) are potential candidates for applications in the aerospace sector, particularly for hypersonic vehicles, reusable launch vehicles, etc. Specific examples that demand the above properties include wing leading edges, engine cowl inlets, nose-caps, etc. Low density of SiC makes it a light-weight alternative for re-entry vehicle applications and components used in the propulsion systems of rockets and satellites [1]. Though the blanks are pressed to near net shape, most of them undergo secondary operations such as drilling, milling etc. These materials have high hardness and are difficult to machine by conventional methods and demands a non-traditional machining method for effective material removal. Other ceramics like Si_3N_4 were found to have properties similar to SiC and Si_3N_4 ceramics were doped with TaN, carbon nanotubes (CNT), $MoSi_2$, TiN etc. to improve electrical conductivity, fracture toughness and thereby improve the machining properties. These electroconductive ceramics replaced many metals in electrical and electronic industry [2–5]. But Si_3N_4 was found to decompose at temperatures above 1600 °C, whereas SiC remained stable up to 2500 °C. However, the major limitations of such monolithic ceramics are poor fracture toughness and machinability. One of the methods for improving the toughness of monolithic ceramics is the addition of a second phase with coefficient of thermal expansion higher than the matrix material. This results in residual stress induced toughening in the material. Through this toughening mechanism, SiC

*Corresponding author. Tel.: +91 471 2568428; fax: +91 471 2568462.
E-mail addresses: chakrvarthy@gmail.com, pchakr@gmail.com (P. Chakravarthy).

0272-8842/$ - see front matter © 2013 Elsevier Ltd and Techna Group S.r.l. All rights reserved.
http://dx.doi.org/10.1016/j.ceramint.2013.05.075

composites processed with a second phase like TiB_2 [6–9], TiC [10–12], were found to possess higher toughness as compared to the monolithic material. If the reinforcing phase happens to be an electrical conductor, there is an overall improvement in the electrical conductivity of the composite. This behavior occurs when the reinforcement is present above a threshold level as described by the percolation theory [13–15]. If the composite possesses electrical resistivity below 100 Ω cm it can be amenable to electrical discharge machining [16], which is a cheap and efficient method of processing materials into complex shapes. However, most of non-oxide ceramic reinforcements have poor oxidation resistance above 1000 °C and inferior strength at these temperatures. Considering that the SiC based ceramics have to perform at high temperature in oxidizing environments, the selection of second phase is of prime importance. Transition metal borides and some intermetallic silicides have excellent high temperature stability and can be thought of as reinforcement for SiC without compromising its high temperature performance. These reinforcing materials have very good electrical conductivity and hence can confer sufficient conductivity to the composite when present in sufficient quantity in line with percolation theory. If the electrically conducting reinforcements are present above a threshold level, it can confer sufficient electrical conductivity to the SiC based ceramics thereby making them amenable to electrical discharge machining. This will facilitate shaping the composite to the required geometry without using expensive diamond tools as required for conventional machining. It is reported that addition of 30 vol% ZrB_2 to SiC resulted in significant improvement in electrical conductivity of the composite material as compared to SiC [1]. However, no detailed study to identify the percolation threshold by varying ZrB_2 content was reported and also the EDM machinability of the composite was not demonstrated. Though the room temperature flexural strength of this composite was reported, no data on the high temperature strength is explored. The literature on SiC ceramics with ZrB_2 as reinforcement is very scarce [17–19] and no reports exist on the effect of varying ZrB_2 content (till 30 vol%) on the properties. The effect of ZrB_2 additions in the range of 10–30 vol% on the densification, microstructure, thermal, electrical and mechanical behavior of SiC matrix is investigated and presented in this paper.

2. Experimental procedure

2.1. Powder characterization and preparation

Commercially obtained powders of SiC, ZrB_2, AlN and Y_2O_3 were characterized for particle size distribution and surface area and the details of the powders used are furnished in Table 1. Surface morphology of SiC and ZrB_2 powders was observed using SEM and the micrographs are shown in Fig. 1. SiC and its composites containing 10, 20 and 30 vol% of ZrB_2 with 2.4 vol% AlN and 2.3 vol% Y_2O_3 as sintering additives [20] were wet milled for 8 h with isopropyl alcohol as the medium in Fritch P5 Pulversette planetary ball mill at 180 rpm. The composites of SiC with 10, 20 and 30 vol% ZrB_2 are denoted as SZ10, SZ20 and SZ30 respectively.

2.2. Hot pressing

The dried powder mixtures were hot pressed into a compact of Ø 95 mm (Fig. 2) under vacuum environment in graphite die assembly using a vacuum hot press. The hot pressing was carried out under a pressure of 28 MPa for duration of 0.5 h. The material was heated at a rate of 5 °C till 1500 °C, 3 °C/min till 1650 °C and 2 °C/min till the final required temperature of 1900 °C. Hot pressing pressure of 15 MPa was maintained between 1500 °C and 1650 °C after which the pressure was increased to 28 MPa. Data on the temperature, load, and ram position were acquired during the hot pressing operation. After hot pressing, the load was released and the material was allowed to cool in the furnace to room temperature by switching off the heaters. After cooling to room temperature, the hot pressed blank was removed from the die assembly and further processed into various test blanks.

3. Characterization of hot pressed blanks

3.1. Density

The hot pressed blanks were first ground in a surface grinding machine and then polished using diamond paste to remove the surface contaminations if any during pressing. The bulk density of the blanks was measured using Archimedes' principle and compared with the theoretical density calculated using rule of mixtures. The relative density of the composite was then calculated from measured and theoretical densities.

3.2. Microstructural features

Specimens of size 10 mm × 10 mm × 5 mm were mechanically polished using diamond paste and were analyzed for microstructural features using a Scanning Electron Microscope (Zeiss EVO50). The hot pressed blanks were also characterized for the phase relation using X-ray diffractometer (XRD) of PANalytical Xpert Pro make. The phases in the hot pressed blank was determined using Ni filtered Cu Kα radiation with a 2θ step size of 0.0068° and dwell time of 30 s. The polished specimens, SiC and the composite with 30 vol% ZrB_2 (SZ30) were additionally characterized using Transmission Electron Microscopy (TEM) to understand the nature of grain boundaries present in these materials. For this, samples of Ø 3 mm were sliced from the hot pressed blanks and mechanically polished to 100 μm thickness approximately. Thin foils were machined using ultrasonic disc cutter and the samples were further subjected to ion beam milling to produce electron transparent specimens. The samples were viewed in the Transmission Electron Microscope (JEOL J210) with Energy Dispersive Spectroscopy (EDS) attachment.

Table 1
Details of powders used in the present study.

Powder sample	Impurities (wt%)	Average particle size (μm)	Surface area (m^2/g)	Source
SiC	O: 0.9, Al: 0.03, Ca: 0.002, Fe: 0.005	0.78	13.4	Saint Gobain, Sika FCP 13C
ZrB_2	C: 0.15, O: 0.78, N: 0.13, Fe: 0.058, Hf: 1.68	3.21	1.0	H.C. Starck, Grade B
AlN	C: 0.1, O: 2.5, Fe: 0.005	1.65	7.2	H.C. Starck, Grade C
Y_2O_3	Al: 0.005, Ca: 0.003, Fe: 0.005	1.85	8.2	H.C. Starck, Grade B

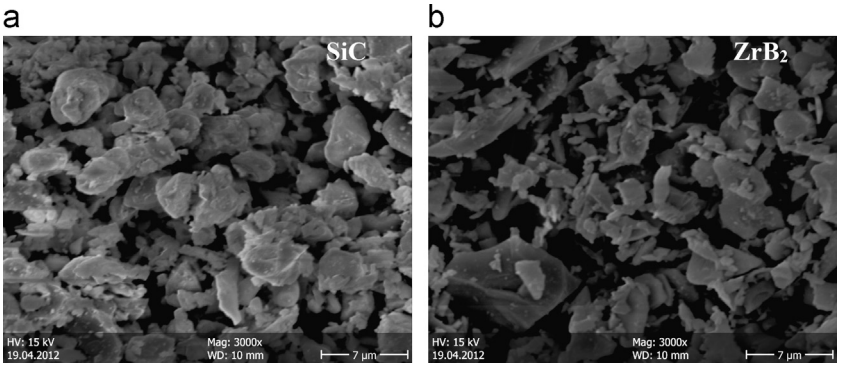

Fig. 1. SEM micrograph of (a) SiC powder and (b) ZrB_2 powders.

Fig. 2. Hot pressed blank.

3.3. Hardness

Shimadzu HMV-2T Hardness Tester was used to measure the Vickers hardness of SiC and its composites. A load of 1 kg was applied for an indentation time of 15 s at ten different locations on the samples. The hardness values were calculated by measuring the mean diagonal lengths of indentations and the average value of hardness is reported.

3.4. Flexural strength

The flexural strength of the SiC, SZ10, SZ20 and SZ30 blanks at room temperature and at 1300 °C was evaluated using 4-point bending test with specimen size of 3 mm × 5 mm × 75 mm in accordance with ASTM C1161. These flexural test specimens were ground using a 400 grit diamond wheel and the tensile surfaces were polished to high degree of finish. The edges were beveled to avoid stress concentration effects during testing. The tests were carried out at a cross head speed of 1 mm/min in an INSTRON MODEL-5582 testing machine in a fully articulating silicon carbide test fixture. Additionally for the high temperature testing, split furnace attachment with $MoSi_2$ heating elements was used and the test was performed in air. Heating rate of 5 °C was used with a 600 s soaking at the test temperature prior to testing. The flexural strength was calculated using the formula

$$\sigma = (3PL)/(4bd^2) \quad (1)$$

where P is the applied load, L is the outer support span, b is the specimen width, and d is the specimen thickness.

The extension of the specimen during test was monitored with Linear Variable Differential Transformer (LVDT) and the stress–strain curve was calculated from this data. A batch of three specimens was tested at each of the temperatures for each material and the average value is reported.

3.5. Thermal diffusivity

Thermal diffusivity (α) of the blanks at room temperature was measured with specimens of size Ø 12.7 mm × 4 mm thickness using the Laser Flash Apparatus according to ASTM E1461-01. The samples were polished to surface finish of 1 μm with diamond paste and given colloidal graphite coating to facilitate absorptivity of the front surface. The specific heat (C_p) values were also obtained in the test and these values are used along with density (ρ) of the materials to calculate the

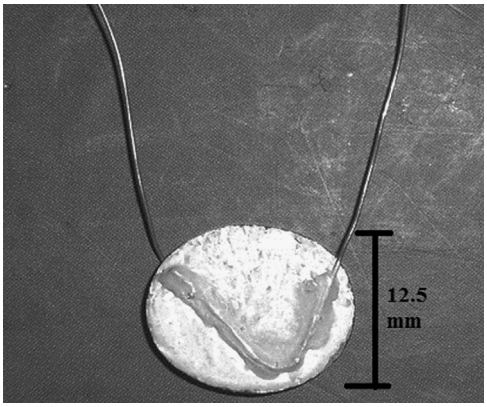

Fig. 3. SiC–ZrB_2 composite sample for AC resistivity measurement.

thermal conductivity (λ) of the material using the formula

$$\lambda = \alpha \rho C_p \quad (2)$$

3.6. Electrical resistivity

3.6.1. Room temperature AC conductivity

Specimens of 1.5 mm thick and Ø 12.5 mm sample were machined and further prepared for testing by applying silver paste on either side and fixing two copper leads to function as electrodes. A typical sample for the measurement is shown in Fig. 3 and the testing was carried out according to ASTM D150 using Quad Tech 7600 plus precision LCR meter. Resistance measurements were made by applying constant voltage.

3.6.2. Room temperature DC resistivity

DC resistivity of SiC and its composites at room temperature was measured by a multi-function calibrator, Fluke 5520 and Digital Multi meter, HP 3458A. The measurement was performed by following ASTM D257 and B63 test methods and using specimens of dimensions Ø 12.5 mm and 1.5 mm thickness. The effect of ZrB_2 on the resistivity of these samples was measured. The measurements were repeated twice on each sample and the average values are reported.

3.7. Electric Discharge Machining

EDM machining of SiC and its composites was attempted with samples of size 3 mm × 5 mm × 50 mm in ELEKTRA PULS S-50 ZNC machine with Ø 12.5 mm copper rod as electrode. A gap voltage of 1 V and sparking current of 5 A were set as process parameters.

4. Results and discussion

4.1. Densification and microstructural features

The relative density achieved in hot pressing for SiC and its composites is shown in Table 2. Though all the material compositions were hot pressed with similar process parameters the density was observed to decrease marginally with increase in the vol% of ZrB_2. The relative difficulty in sintering observed with increasing vol% of ZrB_2 content is attributed to inherent poor sintering characteristics of ZrB_2 material due to its high covalency and also the relatively coarser ZrB_2 particles as compared to SiC used in the present study. The distribution of ZrB_2 in SZ10, SZ20 and SZ30 are shown in the scanning electron micrographs presented in Fig. 4. It can be observed that the bright ZrB_2 grains are uniformly distributed in the SiC matrix. In addition few pores are also visible in the micrographs. The average grain intercept size was measured using *Image J* open source software and the intercept size of SiC was measured to be 1.179 ± 0.5 μm, while the average second phase size in SZ10, SZ20 and SZ30 composites were found to be 3.21 ± 0.58 μm, 3.13 ± 0.51 μm and 3.03 ± 0.63 μm respectively. The XRD patterns of hot pressed SiC, SZ10, SZ20 and SZ30 are shown in Fig. 5 and it can been seen that the processing parameters used here resulted in SiC and the reinforcement phases after hot pressing in addition to YAG phase. The peak intensity of YAG phase formed due to the reaction between the sintering additives during hot pressing in the XRD plots is very weak. With increase in ZrB_2 content, dominant peaks of intensity are essentially that of ZrB_2 owing to its high atomic scattering factor. The XRD results also imply that the reinforcement and the matrix material have good thermochemical compatibility at the processing conditions and no reactions occurred between them. The present work also confirms the results of excellent thermochemical compatibility reported by other researchers. The TEM images of SiC and the composite containing 30 vol% ZrB_2 are shown in Fig. 6. From these images, it can be observed that SiC grains exhibit high stacking faults and there exists a grain boundary phase which is rich in Y, Al, O and Si in addition to some of the impurity elements like Fe. The grain boundary (GB) glassy phase was found to be of about 2.1 nm thickness. The constituents of sintering additives were also found at the triple junctions. In the case of SZ30, film containing the constituents of sintering additives was also observed at grain boundary and triple and multigrain junctions as evidenced by EDS.

4.2. Properties

4.2.1. Hardness

The hardness values of SiC and its composites are shown in Table 2. The hardness of SiC, which was measured to be 23.5 GPa, was found to increase marginally with addition of ZrB_2 as evidenced by the measured values of 24.1, 24.8 and 25.8 GPa respectively for the composites containing 10, 20 and 30 vol% ZrB_2. The improvement in hardness values of composite materials as compared to SiC is attributed to the relatively higher hardness (29.4 GPa) of ZrB_2 material [21] as compared to hardness (24.6 GPa) of pure SiC [1]. The indentation cracks generated were found to propagate in the material. Cracks propagation was not deflected in SiC, but in the composites the cracks were found to be deflected at second phase particles indicating the possibility of toughness

Table 2
Properties of SiC and its composites.

Sample	Relative density (%)	Hardness (GPa)	Flexural strength (MPa)
SiC	99.7	23.5	577.7
SZ10	99.0	24.1	348.0
SZ20	99.3	24.8	261.4
SZ30	97.6	25.8	218.6

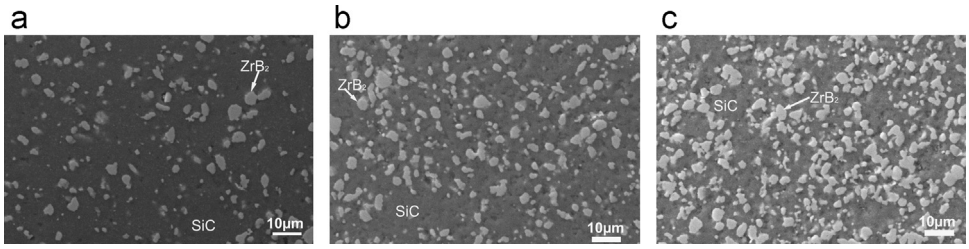

Fig. 4. Scanning Electron Micrographs of (a) SZ10, (b) SZ20 and (c) SZ30.

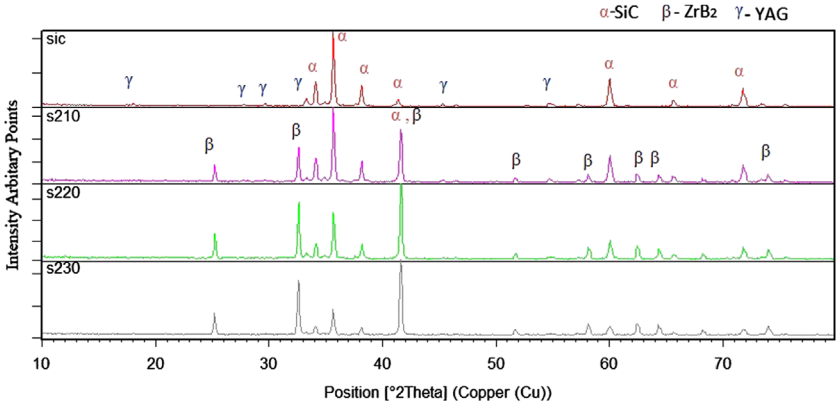

Fig. 5. XRD patterns of hot pressed SiC and its composites.

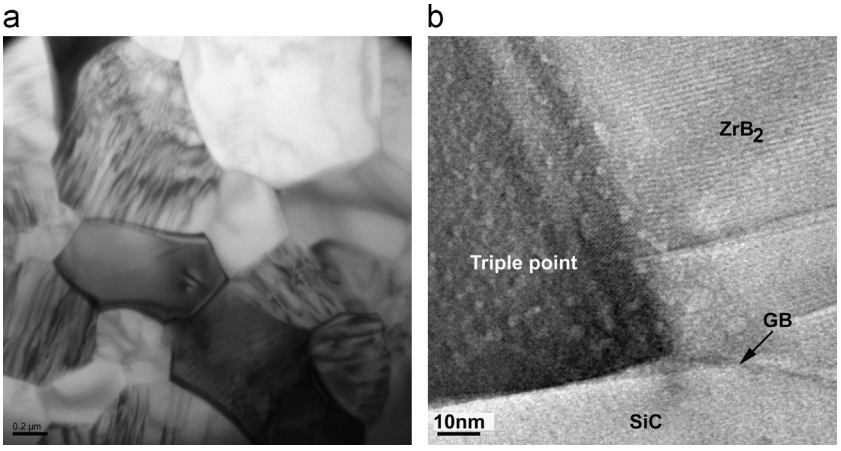

Fig. 6. TEM of (a) SiC and (b) SZ30.

improvement in the composites. Toughening occurs due to the mismatch in the coefficient of thermal expansion of the matrix and reinforcement phases introducing residual stresses. Similar type of behavior is seen in other composite materials also.

4.2.2. Flexural strength

The flexural strength values of SiC and its composites at room temperature and 1300 °C are also shown in Table 2. Against the silicon carbide, the composites containing ZrB_2

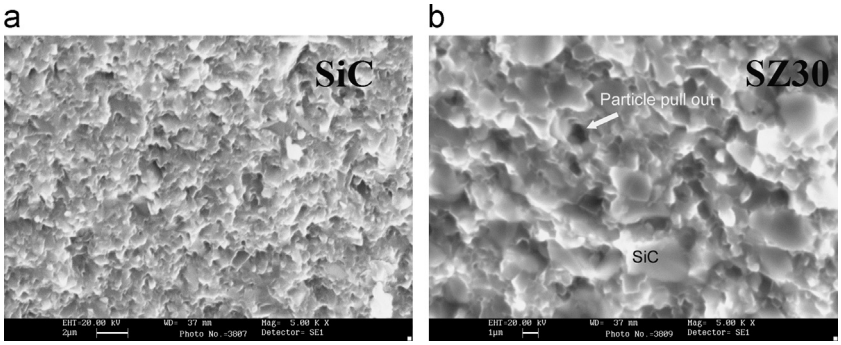

Fig. 7. Fractographs of SiC and SZ30.

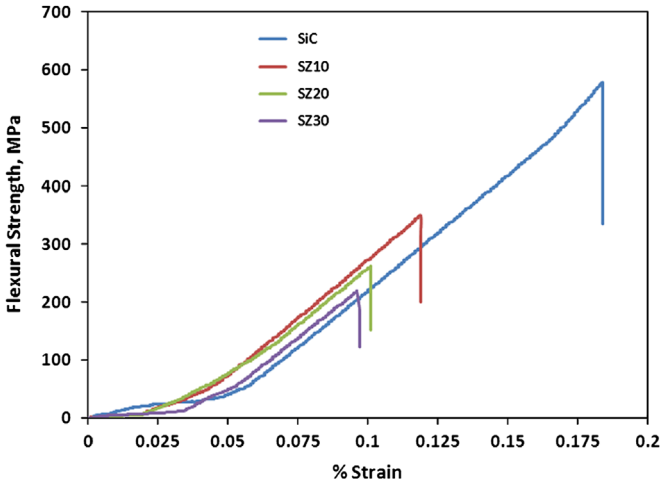

Fig. 8. Stress–strain graph of SiC and its composites.

Table 3
Thermal conductivity of SiC and its composites.

Specimen	Temperature (°C)	Diffusivity (cm^2/s)
SiC	50	0.35
	600	0.13
	1200	0.08
SZ10	50	0.34
	600	0.14
	1200	0.07
SZ20	50	0.30
	600	0.13
	1200	0.08
SZ30	50	0.33
	600	0.14
	1200	0.10

exhibited lower strength. The lower strength of the composites can be attributed to the lower inherent strength of the ZrB_2 material (200–359 MPa) [22]. Also due to the difference in the coefficient of thermal expansions of SiC and ZrB_2, the ZrB_2 particles are expected to remain under tensile residual stresses after cooling from the hot pressing temperature. These tensile stresses will become additive to the stresses due to externally applied load resulting in premature fracture at lower strength. The larger size of the second-phase particles compared to the SiC particles, as evidenced by SEM could also have contributed to the lower strength of the composites. Fractographs of the surfaces of SiC and SZ30 (Fig. 7) reveal the fracture mode to be mainly inter-granular in nature. Particle pull out is clearly observed from the figures in the composite material. It can be visualized from the fracture surface that the grains of SiC are highly strained when compared to the grains in SZ30 sample. This can also be confirmed by the stress–strain graph shown in Fig. 8. From the stress–strain curves it can also be observed that the fracture occurs in a brittle manner with total elastic strain decreasing with increasing ZrB_2 content.

4.2.3. Thermal diffusivity

Thermal diffusivity values of the hot pressed blanks are shown in Table 3. The addition of ZrB_2 did not cause any significant change in the diffusivity of the composites. The diffusivity of polycrystalline SiC might have been reduced marginally due to various factors like random orientation of the grains, lattice impurities, structural defects within grains and secondary phases with poorer conductivity at grain boundaries. It is well known that the thermal transport in ceramic materials predominantly occurs through phonons and the mean free path of phonon transport is affected by the defects, impurities and grain boundary phases as they act as thermal resistance barrier in the material. The diffusivity values decreased at higher temperatures and this can be attributed to phonon–phonon interactions limiting the mean free path of motion of phonons resulting in phonon scattering. The probability of phonon–phonon interactions increases with increasing temperature there by diminishing the thermal diffusivity [23].

4.2.4. Electrical resistivity

Results of AC resistivity measurements at 20 Hz and 1 MHz are presented in Table 4. It can be observed that the addition of ZrB_2 decreases the resistivity at both the frequencies. Electrical conductivity of ceramics varies with the frequency of the applied field and this is due to the fact that charge transport mechanisms are frequency dependent. Variations of phase angle 'θ' with frequency for SiC and its composites are shown in Fig. 9. From the plot it can be observed that the 'θ' value for SiC and SZ10 lies in the region between −25° and −45°,

Table 4
Electrical resistivity values of SiC and its composites.

Sample	AC resistivity at 20 Hz (kΩ cm)	AC resistivity at 1 MHz (kΩ cm)	DC resistivity (kΩ cm)
SiC	393	1.28	2966
SZ10	600	0.83	2771
SZ20	5.52	0.14	1716
SZ30	0.18	0.025	2.095

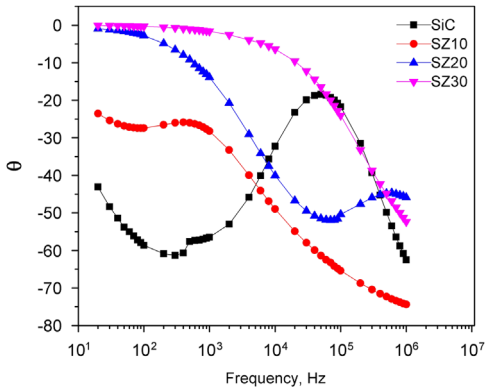

Fig. 9. Variation of phase angle 'θ' with frequency SiC and its composites.

indicating the dominance of the capacitive behavior. In SZ20 and SZ30 composites, the value of 'θ' at lower frequencies approaches zero indicating the dominance of conductive behavior. However, in the region of higher frequency the value of increasing 'θ' shows the dominance of capacitive behavior. This is due to the effect of grain boundaries in the material.

DC Resistivity measurements conducted on SiC and its composites are shown in Table 4. The resistivity is found to decrease with increase in ZrB_2 content. In SZ30, a network of ZrB_2 particles is formed as observed in the micrographs. This enables transport of charge carries through the composite, increasing its conductivity.

4.3. Electric Discharge Machining

An attempt to check the machinabiltiy of all samples using EDM was carried out. SiC, SZ10, SZ20 and SZ30 samples did not respond to EDM owing to their high resistivity. The amount of conductive phase in these materials could not impart sufficient conductivity to enable sparking by EDM. The conductivity of SZ30 was found to be sufficient enough for EDM to be performed and the sample was roughly machined. The sample, before and after machining is shown in Fig. 10.

5. Conclusions

The density of SiC and its composites decreases with increasing ZrB_2 content which can be attributed to poor sinterability of ZrB_2 material due to its high covalence and also the relatively coarser particles compared to SiC.

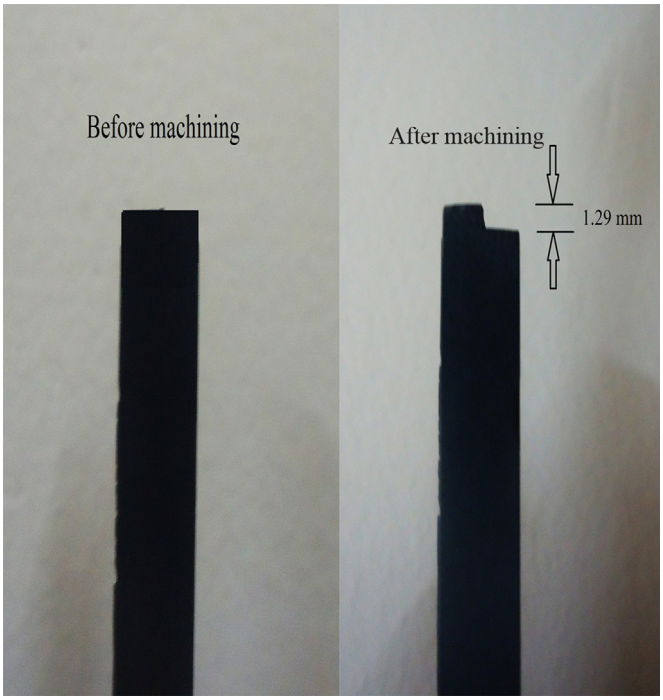

Fig. 10. EDM machined sample of SZ30.

Microstructure revealed the bright ZrB_2 portions that are uniformly distributed and a network of ZrB_2 grains formed in SZ30. The XRD results imply that the reinforcement and the matrix material have good thermochemical compatibility at the processing conditions and no reactions occurred between them. SiC and its composites with ZrB_2 exhibited improved hardness ranging from 23.5 GPa for SiC to 25.8 GPa for SZ30. The composites of SiC with ZrB_2 exhibited lower flexural strength of 218 MPa for SZ30 when compared to 577 MPa of SiC. The lower strength of the composites can be attributed to the lower inherent strength of the ZrB_2 reinforcement and more importantly to the residual tensile stresses in the reinforcement particles. Addition of ZrB_2 was found not to have significant effect on the thermal diffusivity of SiC. Thermal diffusivity of SiC and its composites with ZrB_2 were found to decrease with increasing temperature up to 1200 °C. Addition of ZrB_2 decreased resistivity which further decreased with increase in frequency. Minimum resistivity values of 0.177 kΩ cm and 25.2 Ω cm were measured for SZ30 at 20 Hz and 1 MHz respectively. DC resistivity data at room temperature also

showed the decreasing trend of resistivity with increase in ZrB_2 content. SZ30 composite showed a least resistivity of 2.095 kΩ cm. A network of ZrB_2 particles is formed in this composite as observed in micrographs enabling transport of charge carries through the composite and thereby increasing its conductivity. SiC, SZ10, SZ20 samples did not respond to EDM, considering their high resistivity. The amount of ZrB_2 in these samples could not impart sufficient conductivity to enable machining by EDM, whereas SZ30 sample could be machined due to its low resistivity.

References

[1] R. Suresh Kumar, D. Sivakumar, Ashutosh S. Gandhi, Processing and properties of silicon carbide and its composites containing $MoSi_2$ and ZrB_2, Materials Science and Engineering A 540 (2012) 107–114.

[2] Vitaly Y. Petrovsky, Zbigniew S. Rak, Densification, microstructure and properties of electroconductive Si_3N_4–TaN composites, Journal of the European Ceramic Society 21 (2001) 219–235.

[3] Csaba Bala´zsi, Bala´zs Fe´nyi, Development of CNT/Si_3N_4 composites with improved mechanical and electrical properties, Composites Part B 37 (2006) 418–424.

[4] K. Yamada, N. Kamiya, High temperature mechanical properties of Si_3N_4–$MoSi_2$ and Si_3N_4–SiC composites with network structures of second phases, Materials Science and Engineering A 261 (1999) 270–277.

[5] Lian Gao, Jingguo Li, Takafumi Kusunose, Preparation and properties of TiN–Si_3N_4 composites, Journal of the European Ceramic Society 24 (2004) 381–386.

[6] M.A. Janney, Mechanical properties and oxidation behavior of a hot pressed SiC–15 vol% TiB_2 composite, American Ceramic Society Bulletin 66 (1987) 322–324.

[7] C. Blanc, F. Thevenot, D. Treheux, Wear resistance of α SiC–TiB_2 composites prepared by reactive sintering, Journal of the European Ceramic Society 19 (1999) 571–579.

[8] D. Bucevac, S. Boskovic, B. Matovic, V. Krstic, Toughening of SiC matrix with in-situ created TiB_2 particles, Ceramics International 36 (7) (2010) 2181–2188.

[9] Kyeong-Sik Cho, Heon-Jin Choi, June-Gunn Lee, Young-Wook Kim, In situ enhancement of toughness of SiC–TiB_2 composites, Journal of Materials Science 33 (1998) 211–214.

[10] H. Endo, M. Ueki, H. Kubo, Microstructure and mechanical properties of hot-pressed SiC–TiC composites, Journal of Materials Science 26 (1991) 3769–3774.

[11] Jing Chen, WenJun Li, Wan Jiang, Characterization of sintered TiC–SiC composites, Ceramics International 35 (2009) 3125–3129.

[12] J. Cabrero, F. Audubert, R. Pailler, Fabrication and characterization of sintered TiC–SiC composites, Journal of the European Ceramic Society 31 (3) (2011) 313–320.

[13] Scott Kirkpatrick, Percolation and conduction, Reviews of Modern Physics 45 (1973) 574–588.

[14] D. Bergman, Electrical transport properties near a classical conductivity or percolation threshold, Physica A 157 (1989) 72–78.

[15] D.S. McLachlan, M. Blaszkiewicz, R.E. Newnham, Electrical resistivity of composites, Journal of the American Ceramic Society 73 (1990) 2187–2203.

[16] W. König, D.F. Dauw, G. Levy, U. Panten, EDM—future steps towards the machining of ceramics, CIRP Annals—Manufacturing Technology 37 (1988) 623–631.

[17] H. Tanaka, N. Iyi, Polytypes, grain growth and fracture toughness of metal boride particulate SiC composites, Journal of the American Ceramic Society 78 (1995) 1223–1229.

[18] Jung-Hoon Lee, Jin-Young Ju, Cheol-Ho Kim, Jin-Hyoung Park, Hee-Seung Lee, Yong-Deok Shin, The development of an electroconductive SiC–ZrB_2 composite through spark plasma sintering under argon atmosphere, Journal of Electrical Engineering and Technology 5 (2010) 342–351.

[19] Jin-Young Ju, Cheol-Ho Kim, Jae-Jin Kim, Jung-Hoon Lee, Hee-Seung Lee, Yong-Deok Shin, The development of an electroconductive SiC–ZrB_2 ceramic heater through spark plasma sintering, Journal of Electrical Engineering and Technology 4 (2009) 538–545.

[20] R. Suresh Kumar, Development of Silicon Carbide Based Materials for Aerospace Applications, Ph.D. Thesis, 2012.

[21] Lars Bsenko, Torsten Lundström, The high-temperature hardness of ZrB_2 and HfB_2, Journal of the Less Common Metals 34 (2) (1974) 273–278.

[22] A.L. Chamberlain, W.G. Fahrenholtz, G.E. Hilmas, D.T. Ellerby, Characterisation of zirconium diboride for thermal protection systems, Key Engineering Materials 264–268 (2004) 493–496.

[23] P.G. Klemens, Thermal conductivity of dielectric solids at low temperatures, Proceedings of the Royal Society of London A208 (1951) 108–133.